DOI:
10.1063/1.5024850

Document Version
Publisher's PDF, also known as Version of record

On the solvation of the phosphocholine headgroup in an aqueous propylene glycol solution

Natasha H. Rhys, Mohamed Ali Al-Badri, Robert M. Ziolek, Richard J. Gillams, Louise E. Collins, M. Jayne Lawrence, Christian D. Lorenz, and Sylvia E. McLain

Citation: The Journal of Chemical Physics **148**, 135102 (2018); doi: 10.1063/1.5024850
View online: https://doi.org/10.1063/1.5024850
View Table of Contents: http://aip.scitation.org/toc/jcp/148/13
Published by the American Institute of Physics

On the solvation of the phosphocholine headgroup in an aqueous propylene glycol solution

Natasha H. Rhys,[1] Mohamed Ali Al-Badri,[2] Robert M. Ziolek,[2] Richard J. Gillams,[1,3] Louise E. Collins,[4] M. Jayne Lawrence,[5,a)] Christian D. Lorenz,[2,b)] and Sylvia E. McLain[1,c)]

[1]*Department of Biochemistry, University of Oxford, Oxford OX1 3QU, United Kingdom*
[2]*Department of Physics, King's College London, London WC2R 2LS, United Kingdom*
[3]*Earth-Life Sciences Institute, Tokyo Institute of Technology, Meguro-ku, Tokyo 152-8550, Japan*
[4]*Department of Pharmaceutical Sciences, King's College London, London SE1 9NH, United Kingdom*
[5]*Division of Pharmacy and Optometry, University of Manchester, Manchester ML13 9PL, United Kingdom*

(Received 5 February 2018; accepted 13 March 2018; published online 3 April 2018)

The atomic-scale structure of the phosphocholine (PC) headgroup in 30 mol. % propylene glycol (PG) in an aqueous solution has been investigated using a combination of neutron diffraction with isotopic substitution experiments and computer simulation techniques—molecular dynamics and empirical potential structure refinement. Here, the hydration of the PC headgroup remains largely intact compared with the hydration of this group in a bilayer and in a bulk water solution, with the PG molecules showing limited interactions with the headgroup. When direct PG interactions with PC do occur, they are most likely to coordinate to the $N(CH_3)_3^+$ motifs. Further, PG does not affect the bulk water structure and the addition of PC does not perturb the PG-solvent interactions. This suggests that the reason why PG is able to penetrate into membranes easily is that it does not form strong-hydrogen bonding or electrostatic interactions with the headgroup allowing it to easily move across the membrane barrier. *Published by AIP Publishing.* https://doi.org/10.1063/1.5024850

I. INTRODUCTION

Although water is the most commonly used pharmaceutical solvent, it can be beneficial to either partially or completely replace it with a water miscible polar solvent. 1,2 propandiol or propylene glycol (PG) is the most frequently used co-solvent or replacement solvent, where it has been widely used for over 50 years not only as a pharmaceutical excipient, most often in oral solutions, aerosols and parenteral, and topical preparations, but also as a humectant and as a preservative.[1] Because of its low toxicity, PG is included in the US Food and Drug Agency (FDA) Inactive Ingredients Database, and its use as an excipient is documented in the three main Pharmacopeias, namely, that of the United States, Europe, and Japan. Further to its pharmaceutical use, PG is also extensively used as a food additive, for example, in Europe, it is E1520,[1] while in the US, it is generally regarded as safe (GRAS) by the FDA. Furthermore, the Centre for the Evaluation of Risks to Human Reproduction (NTP-CERHR Monograph, 2004) in its National Toxicology Program reported negligible concern for adverse effects from PG on development and reproduction.

Despite its widespread use, relatively little is known about the interaction of PG with biological molecules, where importantly PG must interact with cellular membranes in order to aid in effective drug delivery *in vivo*. The interaction between PG and the lipids which comprise a significant component of biological membranes is not well understood. Reports in the literature suggest that PG preferentially solvates the lipid headgroup,[2] and *in vitro* PG destabilizes the lamellar structure in bilayers where it promotes the formation of an isotropic phase at temperatures above that of the gel-to-liquid phase transition temperature.[3] The use of a PG in some liposomal preparations yields propylene glycol-embodying liposomes which show increased drug entrapment and greater skin permeability.[4] Further, investigations on cholesterol-containing lamellar phases of distearoylphosphatidylcholine show an increased stability in water/PG solutions.[5] Conversely, variable aggregation of surfactant molecules has been observed in aqueous PG solutions, with the degree of aggregation observed attributable to the dielectric constant of both the surfactant headgroup and to the solvent environment.[6] The ability of PG to promote permeability and stabilization is undeniably connected to the interactions of the solvent environment with functional groups on the lipid, particularly the headgroup.

Although it is known that PG can alter the behavior of lipids *in vitro*, it is still not understood how this occurs in solution, particularly with respect to the atomic-scale interactions that necessarily occur between the atoms on the lipids and both the surrounding water and PG molecules in the solution. Uncovering the details of these interactions can help aid in a better understanding of the interplay between water and PG, as well as how PG affects the hydration of lipid headgroups and vice versa. In the current work, the atomic scale structure of the phosphatidylcholine (PC) lipid headgroup

[a)]jayne.lawrence@manchester.ac.uk
[b)]chris.lorenz@kcl.ac.uk
[c)]sylvia.mclain@bioch.ox.ac.uk

of 1,2-dipropionyl-*sn*-glycero-3-phosphocholine (C_3-PC) in aqueous (30 mol. %) PG solutions has been investigated in order to elucidate the fundamental interactions between water, PG, and the PC headgroup. This work was performed using a combination of neutron diffraction enhanced by isotopic substitution (NDIS) and computational techniques, namely, Empirical Potential Structure Refinement (EPSR)[7] and Molecular Dynamics (MD) where these techniques used in conjunction can provide detailed information concerning the hydration structure and the disruption thereof around biological molecules in solution.[8–15]

II. METHODS

A. Neutron diffraction

Neutron diffraction using isotopic substitution (NDIS) enhanced by computer simulation is one of the premier techniques to understand the hydration of molecules on the atomic scale in solution.[8–23] Neutron diffraction experiments have been used to study an aqueous solution of 30 mol. % PG, containing 200 mM of 1,2-dipropionyl-*sn*-glycero-3-phosphocholine (C_3-PC). The neutron diffraction experiments were performed on the SANDALS diffractometer at the ISIS neutron facility, UK. As the signal for hydrogen and deuterium differs, with a coherent scattering length of −3.76 fm and 6.67 fm, respectively,[24] isotopic substitution experiments can be used to differentiate groups within the system, where the scattering signal arising from any given correlation will differ as a function of the isotopic labeling. A total of 6 isotopomers of the solution were measured (Table I), where both the water and the PG solvent had variable levels of deuteration. To prepare the samples, 1,2-propanediol-h_8 (PG-H_8) and 1,2-propandiol-d_8 (PG-D_8), each 98% purity and as a racemic mixture of R- and S- isomers, were purchased from Sigma-Aldrich and used without any further purification. C_3-PC was obtained from Avanti Polar Lipids, Inc., and the sample was prepared by weight using 99.9% deuterium oxide from Sigma-Aldrich, and milliQ water for the samples containing H_2O.

All samples were placed in containers constructed of Ti/Zr alloy, holding a liquid volume of 1.5 ml, and were measured for ∼8 h (∼1000 μA) each, in addition to measuring the empty cans, background, and a vanadium standard for background correction and normalization of the diffraction data. All of the data were corrected for multiple and inelastic scattering and absorption effects using the software Gudrun.[25]

TABLE I. Isotopomers of C_3-PC/PG/water solutions measured by neutron diffraction.

Sample number	PG	Water
I	PG-H_8	H_2O
II	PG-D_8	H_2O
III	PG-D_8	HDO
IV	PG-H_8	D_2O
V	50% PG-H_8: 50% PG-D_8	D_2O
VI	PG-D_8	D_2O

A neutron diffraction experiment gives, after the appropriate corrections, the total static structure factor, $F(Q)$, which is the sum of all pairwise correlations $S(Q)$ in reciprocal space

$$F(Q) = \sum_{\alpha,\beta\geq\alpha} (2-\delta_{\alpha\beta}) c_\alpha\, c_\beta\, b_\alpha\, b_\beta\, (S_{\alpha\beta}(Q)-1). \quad (1)$$

For atoms α and β, b is the coherent scattering length and c is the concentration of each and $S_{\alpha\beta}(Q)$ is related to this real space distances through Fourier transformation viz

$$S_{\alpha\beta}(Q) = 1 + \frac{4\pi\rho}{Q}\int r\,[(g_{\alpha\beta}(r)-1)]\,\sin(Qr)\,\mathrm{d}r, \quad (2)$$

where ρ is the atomic density of the solution in atoms/Å^3 and $g(r)$ is the radial distribution function, which describes how the density of β changes around α with respect to distance, r (in Å). Integration of the $g(r)$ function over a distance range of r_1 to r_2 gives the coordination number, $n(r)$; the number of β atoms around α,

$$n_\alpha^\beta = 4\pi\rho c_\beta \int_{r_1}^{r_2} r^2 g_{\alpha\beta}(r)\,\mathrm{d}r. \quad (3)$$

B. Empirical potential structure refinement

Unlike simple systems with few atomic components where the nearest neighbor $g(r)$s can be extracted solely from the experimental data,[26] more complex systems such as those measured here require computational modeling to extract all of the pairwise interactions in the system. Empirical Potential Structure Refinement (EPSR) modeling[7] can be used to create a model that "fits" the measured diffraction data and has been used for a variety of systems to gain a better understanding of the structure of molecules in solution.[11–14,19–22] EPSR is a Monte Carlo-based simulation which begins with a set of established potentials and then refines these potentials iteratively until a good fit between the measured data and the model is achieved. The EPSR simulation box here contained 10 C_3-PC lipids, 750 PG molecules (375 R- and 375 S-), and 1750 water molecules (Fig. 1). Parameters from the CHARMM force field[27,28] were used as seed potentials for the lipids and PG molecules and SPC/E potentials[29] for the water molecules. The final $F(Q)$ fit of the EPSR simulation to the neutron diffraction data is presented in Fig. 2(a). A Fourier transform, $G(r)$, of these data portrays this information in real-space, which is presented in Fig. SI.1(a) of the supplementary material.

C. Molecular dynamics

Molecular Dynamics (MD) simulations using the CHARMM36 force field[27,28] were performed, providing an independent assessment of the lipid-PG-water solution at the same concentration as the NDIS experiments. Specifically, the MD simulation contained 10 C_3-PC molecules, 750 PG molecules (375 R- and 375 S-), and 1750 water molecules. The water molecules were modeled using TIP3P[30] and all of the hydrogen-containing bonds and the water molecule angles

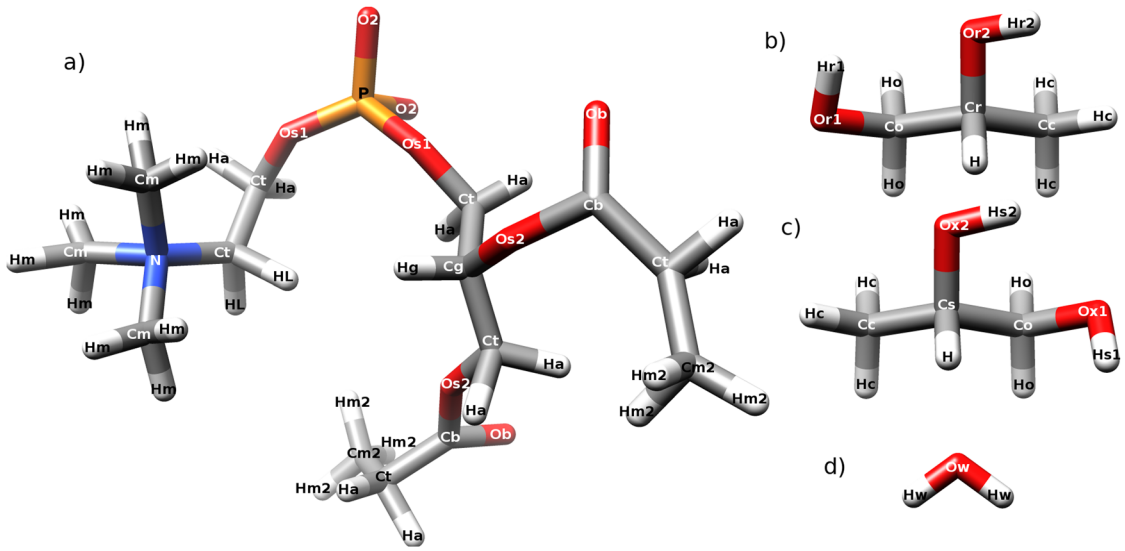

FIG. 1. Molecular structures of (a) C_3-PC, (b) R-PG, (c) S-PG and (d) water with the atomic labels used in the EPSR simulation.

were constrained using the SHAKE algorithm.[31] The volume of the system was equilibrated at 300 K and 1 atm using the NPT ensemble for approximately 1 ns, the subsequent production simulations were performed using the NPT ensemble at 300 K and 1 atm and run for 100 ns. All simulations were conducted using the LAMMPS MD code[32] and a 2.0 fs time step with the velocity Verlet integrator was used and the Nosé-Hoover thermostat and barostat as they are implemented in LAMMPS were used. The van der Waals interactions were cut-off at 12 Å, and the PPPM algorithm[33] was used to compute the long-range Coulombic interactions. The $F(Q)$s calculated from the MD simulation compared to the measured NDIS data are shown in Fig. 2(b), whilst the Fourier transformation of the simulated $F(Q)$ is shown in Fig. SI.1(b) of the supplementary material.

D. Topological analysis

In order to define the topology of the solvents around the various regions of the lipids, a graph-theoretic approach has been used, which represents the structure of a network as a set of nodes V connected by a corresponding set of edges E. Here, nodes represent individual molecules in the simulated system and edges are assigned by an empirical hydrogen bonding measure as defined by Luzar and Chandler.[34] An ensemble of undirected graphs is considered to represent the resulting hydrogen bonding network. Through this formalism, the network structure can be conveniently described by an adjacency matrix $\mathbf{A}$ where $A_{ij} = 1$ if nodes i and j are connected and $A_{ij} = 0$ if nodes i and j are not connected, and $A_{ii} = 0\ \forall i$ since intramolecular hydrogen bonds are not

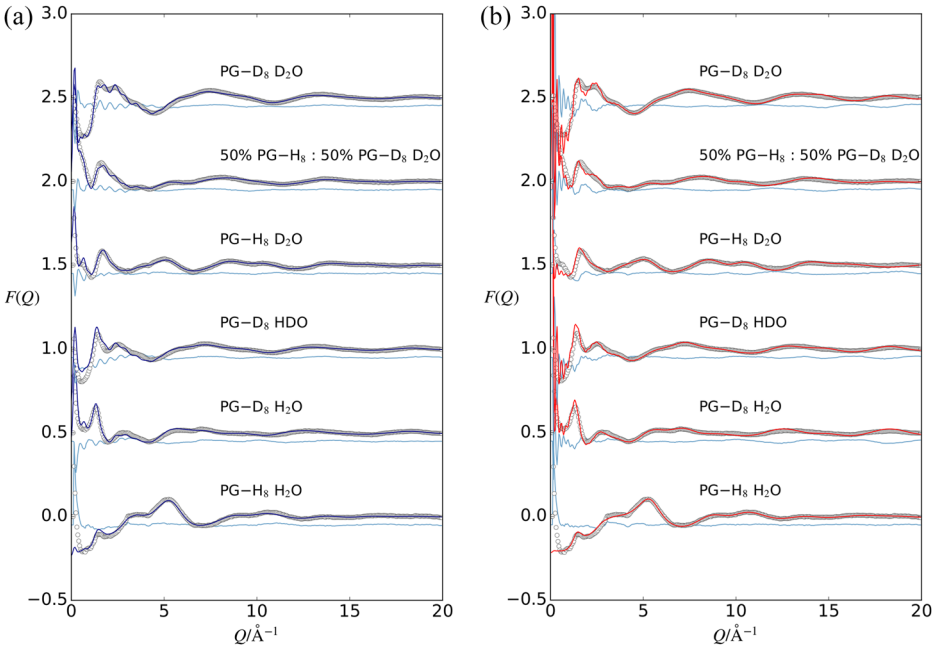

FIG. 2. The $F(Q)$ fits to the measured neutron diffraction data (grey circles) for each isotopomer solution of C_3-PC/PG/water, for (a) EPSR (blue line), and (b) MD (red line) simulations. The pale blue lines show the difference between the fit and the experimental data. Each dataset has been separated by 0.5 for clarity.

considered. An algorithm developed in-house, using some functionality of the *NetworkX* python library,[35] was used to determine the shortest through-water hydrogen bond chains that connect lipid onium, phosphate, and ester groups to each PG molecule.

E. ANGULA

To compliment the $g(r)$ representations of the interactions in this system, the arrangement of PG and water molecules around the functional groups of C_3-PC was obtained from the EPSR and MD simulations using the software ANGULA.[36,37] For this analysis, orthonormal coordinates have been assigned to specific functional groups on C_3-PC, water, and PG. For C_3-PC, coordinate systems were centered on the -$N(CH_3)_3^+$ nitrogen, the adjacent —CH_2— carbon (Ct), the phosphate (P), and the ester group carbon (Cb) atoms, while the coordinate systems were centered on the hydroxyl oxygen atoms for PG and water molecules (see Fig. 2 of the supplementary material) in order to assess the nearest neighboring solvent molecules to specific sites on C_3-PC. By accumulating ~5000 different snapshots of the simulation box for EPSR and trajectories for MD, the distribution of the nearest neighbor contacts, for each group in C_3-PC, has been plotted as a Spatial Density Map (SDM). The density in such SDMs depicts the positions where molecules can be found around a given group,[37,38] where the scale bar represents the local number density of the nearest neighbor contacts, normalized to the number of simulated lipid molecules.

III. RESULTS AND DISCUSSION

A. Solvent structure

Figure 3 shows the water-water and PG-water interactions (for the R-isomers of PG) in the C_3-PC/PG/water system for both EPSR fits to the neutron data and the MD simulation in the form of radial distribution functions, and Table II shows the nearest neighbor coordination numbers for these functions. The corresponding functions for the S-isomers, which are virtually identical, for each simulations are presented in the supplementary material. The hydrogen-bonding interactions between the PG hydroxyl groups with water molecules and water molecules with themselves suggest that the hydrogen bonds have similar strength to one another as they all show a sharp first peak at 1.86 Å. The relative intensity of the peaks observed in these functions can be attributed to local density effects, or excluded volume effects where this has been previously observed for aqueous PG in the absence of C_3-PC at the same concentration,[16] and for acetone and dimethyl sulfoxide (DMSO) in aqueous solutions.[39] The coordination numbers in Table III indicate that EPSR fits to the neutron data show slightly increased water-water coordination and slightly reduced PG-water interactions compared to the MD simulation. In addition, the PG-water coordination numbers are comparable to the degree of hydrogen bonding in aqueous PG at the same concentration.[16] Overall, there are only minor changes to the structure of this solution, suggesting that PC does not perturb the solution, in either simulation.

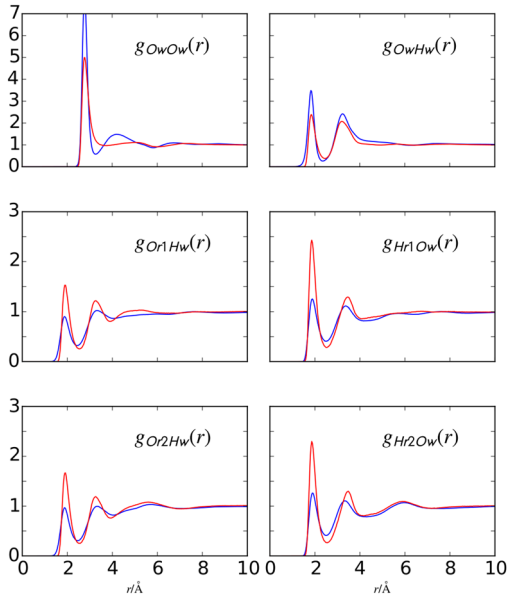

FIG. 3. The $g(r)$s for water-water and PG-water interactions from the EPSR (blue line) and MD (red line) simulations.

B. Solvation of the onium group

Figure 4(a) shows the $g(r)$s for water and PG hydroxyl solvation (from the R-isomer, the S-isomer-PC interactions are shown in the supplementary material) around the —$N(CH_3)_3^+$ (onium group) on C_3-PC for both EPSR and MD, and Table III shows the coordination numbers for these functions. The appearance of the curves and the coordination numbers are virtually identical for both simulations. Overwhelmingly, the coordination of water to the onium group is much higher than that of the hydroxyl groups. Further, the $g_{NOw}(r)$ shows a broad hydration peak at ~4.2 Å in both simulations, similar to what is observed for the hydration of this motif in pure water.[12] Similar to C_3-PC in DMSO/water solutions,[11] the nitrogen is closer to the water oxygens than the PG-hydroxyl oxygens, indicating a comparatively stronger interaction with the water molecules. Compared to C_3-PC in pure water,[12] the coordination number for the N—Ow interaction for EPSR has decreased around 50% from 18.6 to 10.1, which is somewhat expected given that there are two hydroxyl groups for every PG molecule, and at a 30 mol. % concentration, this level of substitution might be expected.

A comparison of the coordination numbers in Table III for the $g(r)$s in Fig. 4(a) shows that PG has a lower propensity

TABLE II. Coordination numbers for the water-water and PG-water $g(r)$s shown in Fig. 3.

$g_{\alpha\beta}(r)$	EPSR (n_α^β)	MD (n_α^β)	r_2 (Å)
Ow–Ow	2.7	2.5	3.30
Ow–Hw	1.3	1.1	2.40
Hw–Hw	3.2	3.0	3.00
Or1–Ow	0.6	0.8	2.50
Hr1–Ow	0.4	0.6	2.50
Or2–Ow	0.6	0.8	2.50
Hr2–Ow	0.4	0.6	2.50

TABLE III. Coordination numbers for the onium-water $g(r)$s shown in Fig. 4.

$g_{\alpha\beta}(r)$	EPSR (n_α^β)	MD (n_α^β)	r_2 (Å)
N–Ow	10.1	10.4	5.6
N–Hw	23.0	24.4	6.0
N–Or1	1.2	1.1	5.5
N–Hr1	1.5	1.3	5.7
N–Or2	1.1	1.1	5.5
N–Hr2	1.3	1.4	5.7
N–Ox1	1.4	1.1	5.5
N–Hs1	1.6	1.3	5.7
N–Ox2	1.2	1.1	5.5
N–Hs2	1.4	1.3	5.7

to form hydrogen bonds with the onium group, for instance, the coordination number in EPSR for N—Ow is 10.1 and is only 1.2 for the N—Or1 interaction. This is likely attributable to the fact that as PG is a larger molecule, it cannot easily be packed around this group. Further, the onium-PG coordination numbers in Table III suggest that there are a similar number of Or1 and Or2 atoms surrounding the onium within the first coordination shell. Unlike the R-isomer, which shows a similar coordination, the onium group in the EPSR and MD simulations, there is slightly more discrepancy found between the simulations for the S-isomer [these $g(r)$s in Fig. SI.3 of the supplementary material]. Here, the EPSR simulation predicts that there is enhanced interaction of S-PG with the onium group, suggesting that this isomer shows more favorable packing around this group. However, this preference is small, with a coordination number increase of 0.3 for the EPSR simulation.

Figures 4(b) and 4(c) show the hydration SDMs around the $N(CH_3)_3^+$ group from the EPSR fits to the neutron data and from the MD simulation. In both of these figures, this group is oriented such that one of the methyl carbon atoms is along the z-axis with the nitrogen at the origin. For both simulations, the nearest neighbor water molecules are predominately located between the $—CH_3$ group, with a higher density underneath this group, below the nitrogen—most clearly seen on the cut through projected onto the back panels in Figs. 4(b) and 4(c). This hydration pattern is similar to what has previously been observed for C_3-PC in pure water,[12] water/DMSO solutions,[11,40] and in a hydrated bilayer[41] as well as for the neurotransmitter acetylcholine in aqueous solutions,[42] which gives rise to the nearest neighbor water molecules that are oriented such that they are coordinated to the onium group via $N^+ \cdots$ Ow solvation interactions.

Figures 4(d) and 4(e) show the SDMs for the nearest neighbor hydroxyl groups from the PG R-isomer for both simulations. For these, the heat-map scale bar has been adjusted for visibility (limited to 0.45) and to account for the reduced number of PG molecules. The diffuse solvation patterns in these SDMs suggest that PG interactions with the $N(CH_3)_3^+$ group are highly diffuse, where EPSR fits to the neutron data show a slightly higher density of the nearest neighbor PG molecules compared to MD. For EPSR, there is a slightly

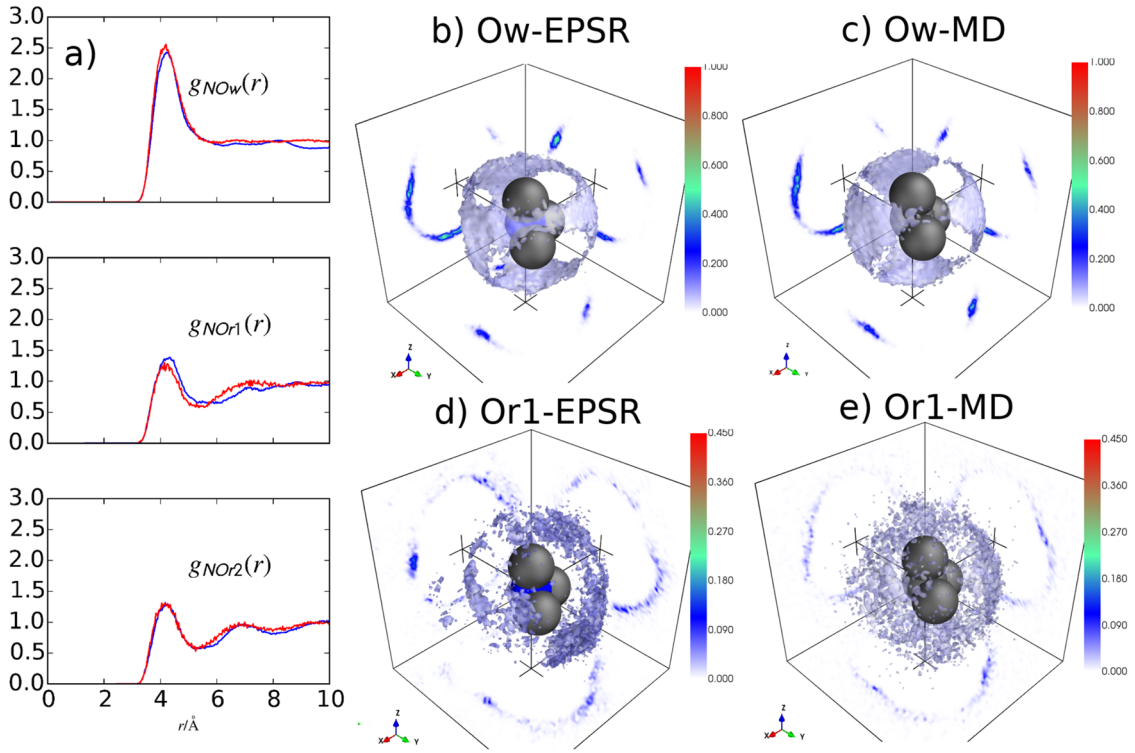

FIG. 4. (a) $g(r)$s for water oxygen (Ow) and the PG hydroxyl oxygens with the $N(CH_3)_3^+$ group on C3-PC, from EPSR (blue line) and MD (red line) simulations. Interactions are shown for the first (Or1) and second (Or2) hydroxyl groups of the R-isomer [S-isomer $g(r)$s are included in the supplementary material]. [(b) and (c)] SDMs for the nearest neighbor water molecules around the onium N from EPSR and MD, respectively. [(d) and (e)] SDMs for the nearest neighbor PG R-isomer Or1 hydroxyl group for EPSR and MD, respectively. The isopycnic surface represents the location of 40% of the nearest neighbor water molecules and 20% of the nearest neighbor PG molecules.

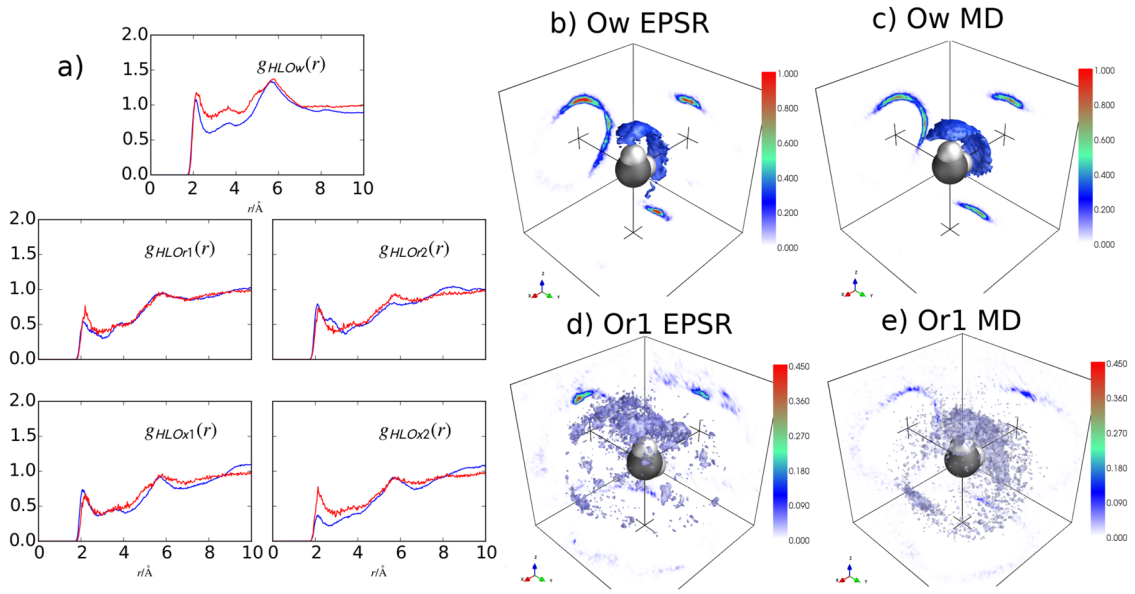

FIG. 5. (a) $g(r)$s for the water oxygen (Ow) and the PG hydroxyl oxygens with the HL atoms on C_3-PC, from EPSR (blue line) and MD (red line) simulations. Interactions are shown for the first (Or1) and second (Or2) hydroxyl groups of the R-isomer [$g(r)$s for the S-isomers are provided in the supplementary material]. [(b) and (c)] SDMs for water molecules around the first $-CH_2$ group for EPSR and MD, respectively. [(d) and (e)] SDMs for the R-isomer first hydroxyl group around the first $-CH_2$ group for EPSR and MD, respectively. The isopycnic surface represents the location of 40% of the nearest neighbor water molecules and 20% of PG nearest neighbor molecules.

increased localized density in the $+x$-direction below the N^+ atom, similar to the hydration seen in Figs. 4(b) and 4(c). Interestingly, the $g(r)$s in Fig. 4 (a) and their respective coordination numbers in Table III suggest that the solvation of this group would be virtually identical between the two simulations, yet the SDMs show a more highly localized coordination of the surrounding solvent, emphasizing the need for 3-dimensional analysis.

Previous hydration studies of the PC headgroup in solution suggested a unique hydrogen-bonding interaction between the methylene group hydrogens (HL; Fig. 1) adjacent to the onium group and the surrounding water solvent.[11,12,41] This hydrogen bonding from water to this portion of the PC molecule is present in the current solutions, as the $g_{\mathrm{HLOw}}(r)$ in Fig. 5(a) in both MD and EPSR fits to the diffraction data show a first peak at around 2.1 Å with a coordination number of ~0.6 hydrogen bonds (Table IV). This value is comparable to that observed in DMSO, where the coordination number was 0.5 for the EPSR simulation,[11] but still exhibits lower coordination of water compared to the 1 bond seen for pure water simulations.[12] Furthermore, the HL-PG-hydroxyl coordination is much lower than the water-HL coordination where there is only around 10% coordination for each hydroxyl group from either isomer.

Figures 5(b) and 5(c) show the SDMs for the nearest neighbor water molecules and Figs. 5(d) and 5(e) show the SDMs for the PG R-isomers around $-CH_2$ below the $N(CH_3)_3^+$ in C_3-PC for both EPSR and MD. It is clear from this figure that there are highly localized water molecules that hydrogen bond with the HL atoms on the methylene groups in both simulations. By contrast, the PG nearest neighbors show a

TABLE IV. Coordination numbers for the H_L-water and H_L-R-PG $g(r)$s shown in Fig. 5.

$g_{\alpha\beta}(r)$	EPSR (n_α^β)	MD (n_α^β)	r_2 (Å)
HL–O*w*	0.6	0.7	2.8
HL–Or1	0.07	0.08	2.8
HL–Or2	0.1	0.09	2.8
HL–Ox1	0.08	0.08	2.8
HL–Ox2	0.04	0.09	2.8

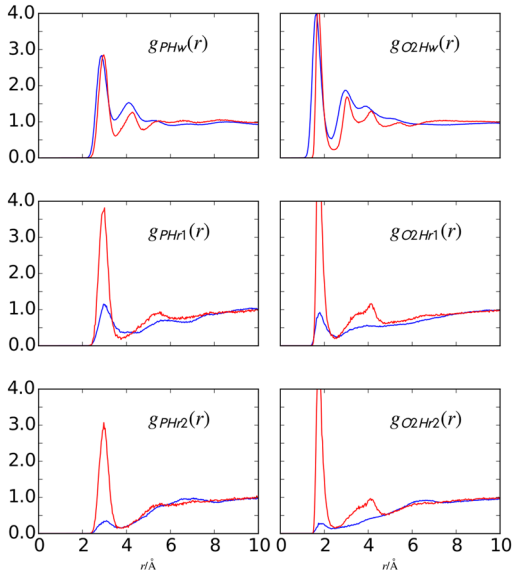

FIG. 6. The $g(r)$s for the water hydrogen (Hw) and the PG hydroxyl hydrogens with the phosphate atom of C_3-PC, from EPSR (blue line) and MD (red line) simulations. Interactions are shown for the first (Hr1) and second (Hr2) hydroxyl groups of the R-isomer [$g(r)$s for the S-isomer are provided in the supplementary material].

diffuse distribution around this —CH_2— portion of the lipid molecule, with the SDM from the MD simulation showing almost no localization of the PG molecules surrounding this methylene group. Interestingly, the Or2 (the central hydroxyl on R-PG; Fig. 1) $g(r)$ [Fig. 5(a)] shows more interactions with this carbon compared to the S-PG isomer in the EPSR fits to the neutron data, concomitant with the highly localized density in the positive z-direction directly above one of the methylene hydrogen sites, which indicates a preference for the R-isomer rather than the S-isomer to be located and receive a hydrogen bond from these methylene hydrogens.

C. Solvation of the phosphate group

Figure 6 shows the $g(r)$s for both water and PG R-isomer hydroxyl solvation of the phosphate group from both simulations [the $g(r)s$ for the S-isomer are in the supplementary material] with the coordination numbers for these functions in Table V. Both EPSR and MD simulations show that water molecules can form direct hydrogen bonds with the phosphate group, through the P═O O2 oxygens, with a hydrogen bonding distance of O2—Hw being 1.65 Å for the EPSR simulation and 1.71 Å for the MD simulation, with each O2 oxygen coordinating approximately 2 Hw atoms. The $g(r)$s for the P—O—C oxygens (Os1; Fig. 1) which show relatively little hydrogen

TABLE V. Coordination numbers for the phosphate-water $g(r)$s shown in Fig. 6.

$g_{\alpha\beta}(r)$	EPSR (n_α^β)	MD (n_α^β)	r_2 (Å)
P–Ow	5.2	4.4	4.5
P–Hw	4.9	4.2	3.5
O2–Ow	2.0	1.6	3.3
O2–Hw	1.8	1.5	2.4
P–Or1	0.3	0.6	4.5
P–Hr1	0.3	0.6	3.9
P–Or2	0.1	0.5	4.5
P–Hr2	0.1	0.5	3.9
O2–Or1	0.07	0.2	3.2
O2–Hr1	0.07	0.2	2.6
O2–Or2	0.03	0.2	3.2
O2–Hr2	0.03	0.2	2.6

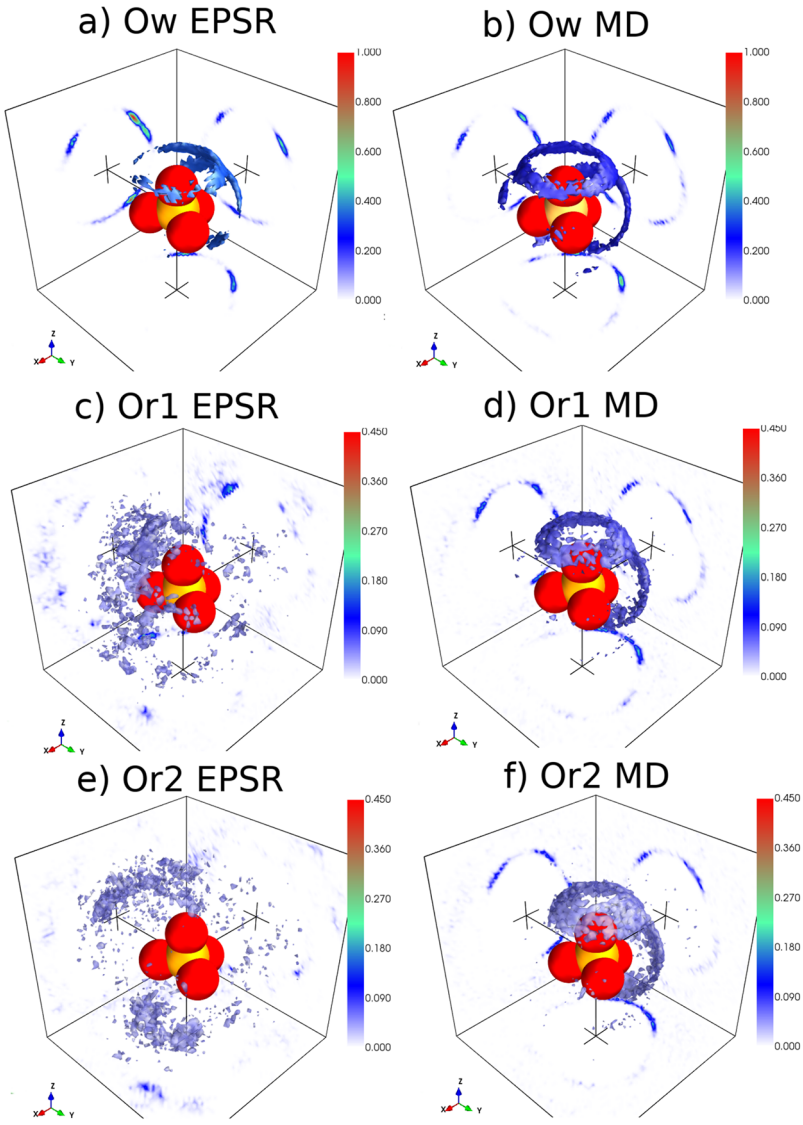

FIG. 7. SDMs for the hydration of the phosphate group from (a) EPSR and (b) MD simulations. The isopycnic surface represents the location of 40% of the nearest neighbor water molecules. SDMs for the PG solvation of the phosphate group through the [(c) and (d)] first hydroxyl and [(e) and (f)] second hydroxyl groups from EPSR and MD, respectively. The isopycnic surface represents the location of 20% of the nearest neighbor PG molecules.

bonding interaction, as expected for these groups,[11,12] are provided in the supplementary material.

In contrast to the $g(r)$s for the onium group (Fig. 4) and the hydration of the PO_4^- group, the $g(r)$s for phosphate-PG interactions from MD simulations in Fig. 6 indicate much more prevalent hydrogen-bonding interaction between O2 and the hydroxyl hydrogens from the PG molecules. The coordination numbers (Table V) show a 2-fold increase in PG-phosphate interactions compared with EPSR fits to the neutron data. The prevalence for hydrogen bonding is still not as strong compared to hydration interactions of this group, but they are marked relative to the EPSR fits to the neutron data.

Figure 7 shows the related SDMs for the hydration for both MD and EPSR fits to the neutron data, where the P═O O2 oxygens are located along the $+z$ and in the $-x$ direction, slightly below the xy-plane. These maps show that the nearest waters have a preference to form a "halo" of density around each P═O (O2) oxygen on C_3-PC and the localized density of cut-throughs on the back panels shows localized hydrogen bonding from the surrounding water solvent to the lone-pairs of electrons on these oxygens. This density is similar for both simulation types with the EPSR-derived SDM showing slightly more localized water positions.

Figure 7 also shows the SDMs for the solvation of the PO_4^- group by both hydroxyl groups on the R-isomer of PG (the S-isomer SDMs are provided in the supplementary material), again for both simulations, where the percentage of molecules shown in these SDMs has been decreased to 20% for clarity. These SDMs account for the difference in EPSR and MD simulations, while the hydroxyl groups bond in the "halo" arrangement for the MD simulation, as seen for the phosphate hydration, the nearest neighbor contacts are diffusely arranged around the phosphate group. This pattern, for each simulation, is observed for both R- and S-enantiomers (see the supplementary material).

D. Solvation of the ester groups

Figure 8 shows the $g(r)$s for the hydration of both the first and second ester group carbonyl oxygens (Ob; Fig. 1) for MD and EPSR fits to the neutron data and the coordination numbers for these are shown in Table VI (the C—O—C oxygen hydration, which is limited, is shown in the supplementary material). It is clear that the MD simulations show a much higher level of hydrogen bonding to this C═O oxygen. This corroborated by the SDMs for the nearest neighbor hydration shown in Figs. 8(b)–8(d) where there is a much higher density of localized hydration around this group in the MD simulation, for

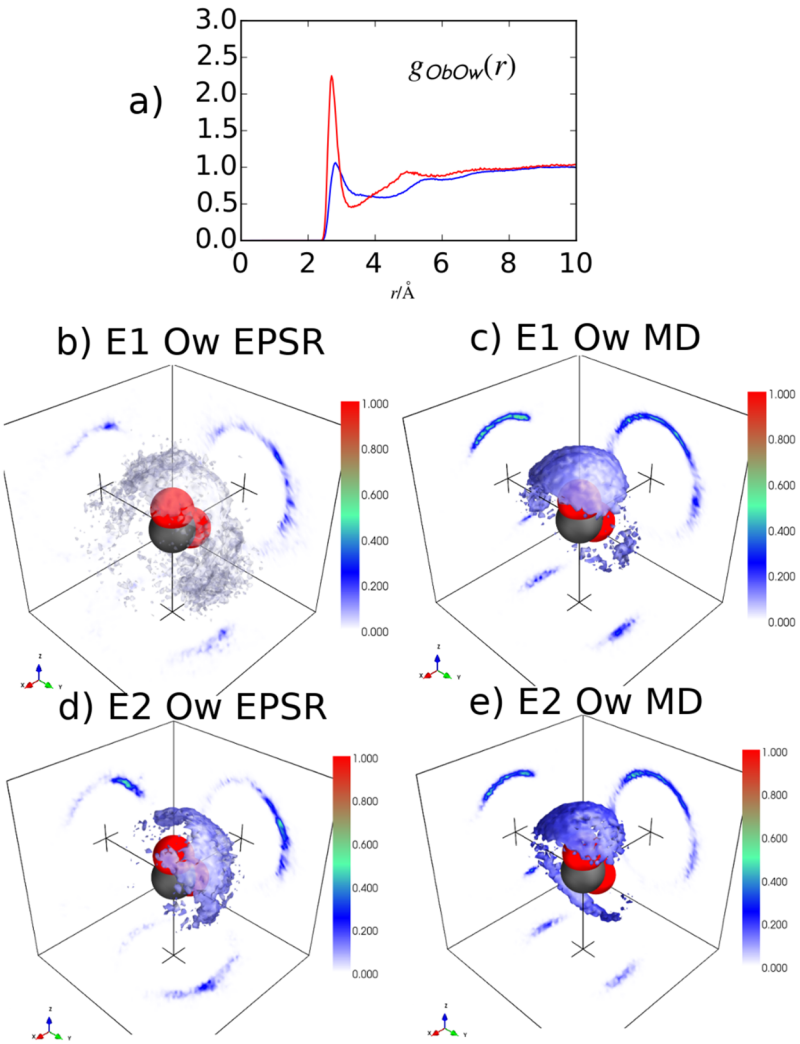

FIG. 8. (a) $g(r)$s for the hydration of the C═O oxygen from the ester groups on C_3-PC from EPSR (blue line) and MD (red line) SDMs for the hydration of the first [(b) and (c)] and second [(d) and (e)] ester groups, where in each case, the isopycnic surface represents the location of 40% of the nearest neighbor water molecules.

TABLE VI. Coordination numbers for the *Ob*-water and *Ob*-PG $g(r)$s shown in Figs. 9–11.

$g_{\alpha\beta}(r)$	EPSR (n_α^β)	MD (n_α^β)	r_2 (Å)
Ob–O*w*	0.8	1.1	3.3
Ob–Or1	0.1	0.1	3.3
Ob–Or2	0.1	0.1	3.3
Ob–Ox1	0.06	0.1	3.3
Ob–Ox2	0.06	0.1	3.3

both ester groups compared with EPSR; most notable for the first ester group where there is a highly diffuse hydration cloud in Fig. 8(b). Interestingly, the two ester groups show different hydration patterns relative to one another in both simulations where EPSR shows less hydrogen bonding in the $+z$ direction compared with MD for the second ester group and there is a further band of high density around the C—O—C oxygen for the MD simulation in Fig. 8(d) that is not as prominent for EPSR. These hydration patterns for both E1 and E2 in C_3-PC are similar to the hydration pattern observed for 1,2-Dioleoyl-sn-glycero-3-phosphocholine (DOPC) in bilayer simulations, where the E2 group shows slightly higher hydration and some density below the C—O—C oxygen atom.[41]

Figure 9 shows the $g(r)$s between the PG hydroxyl oxygens (from both enantiomers) and the ester C=O oxygens (Ob) on the C_3-PC lipid, and Table VI shows the coordination numbers for these functions from both EPSR fits to the neutron data and MD simulation. The lipid C—O—C oxygen-PG $g(r)$s, which show limited hydrogen bonding, are provided in the supplementary material. Similar to the hydration behavior in Fig. 8, MD shows a higher level of hydration around these groups with sharp hydrogen bonding peaks at around 3 Å.

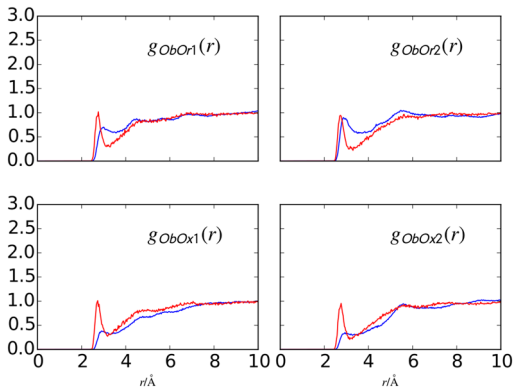

FIG. 9. The $g(r)$s for interactions of the water oxygen (Ow) and PG hydroxyl oxygens with the ester group C=O oxygen (Ob), from the EPSR (blue line) and MD (red line) simulations. Interactions for PG are shown for the first (Or1) and second (Or2) hydroxyl groups of the R-isomer, as well as the first (Ox1) and second (Ox2) hydroxyl groups of the S-isomer.

Figure 10 shows the SDMs for the first hydroxyl nearest neighbor PG molecules (for both enantiomers; Or1 and Ox1 in Fig. 1) around the C=O oxygen of the first ester group in C_3-PC. The first ester group (E1) is the ester connected to the Ct atom on C_3-PC and the second ester group (E2) is the ester connected to the Cg atom on C_3-PC in Fig. 1. In EPSR even though both provide relatively diffuse solvation clouds, the PG R- and S- solvation around C=O look somewhat different to one another. For Or1 [Fig. 10(a)], the PG molecules have some localized density around the Ob atom in pattern which is somewhat reminiscent of the "halo" hydration present around this group in Fig. 8(b) where the R-PG molecules can hydrogen bond to this oxygen. Conversely, for the S-isomers, the solvation density around this C_3-PC E1 group shows the highest localized density below the C=O in the $-z$ direction. It

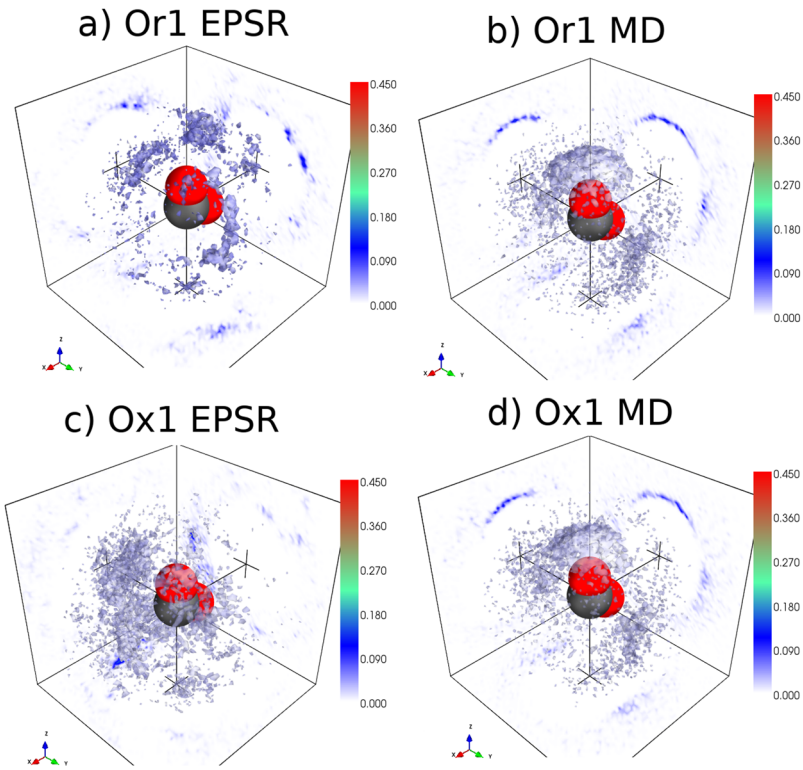

FIG. 10. SDMs for the PG solvation of the first ester group through the R-isomers [(a) and (b)] and S-isomers [(c) and (d)], where in each case, the isopycnic surface represents the location of 20% of the nearest neighbor water molecules.

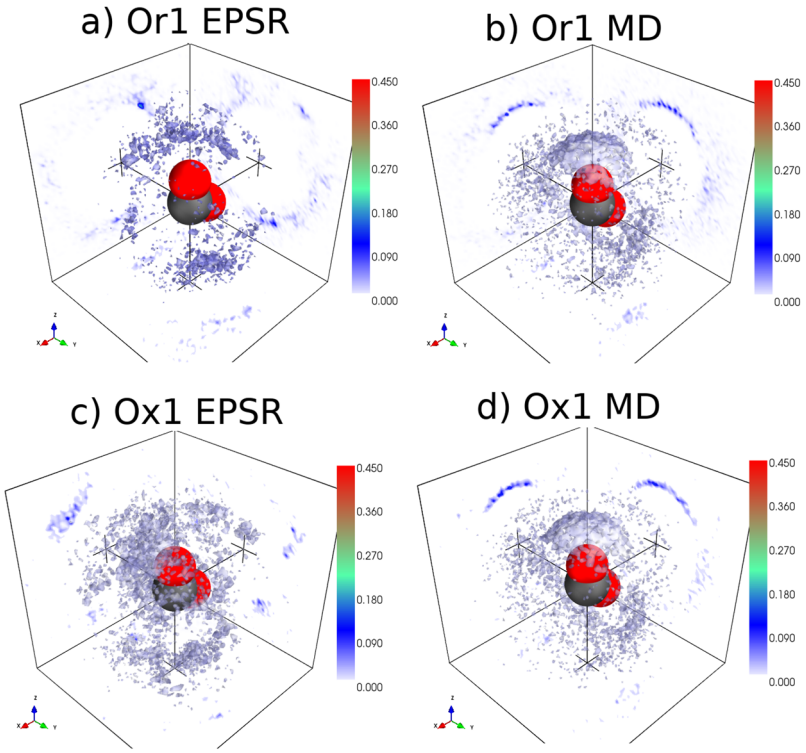

FIG. 11. SDMs for the PG solvation of the second ester group through the R-isomers [(a) and (b)] and S-isomers [(c) and (d)], where in each case, the isopycnic surface represents the location of 20% of the nearest neighbor water molecules.

should be emphasized that in both cases, the density is highly delocalized and as such small increases in the density may just be due to random packing effects. Figures 10(b) and 10(c) show the same functions for MD where in this case there is only solvation density for each of the PG enantiomers where they can hydrogen bond to this E1 Ob atom. In MD, both enantiomers show the same solvation patter around E1 on C_3-PC and more highly localized density compared to EPSR,

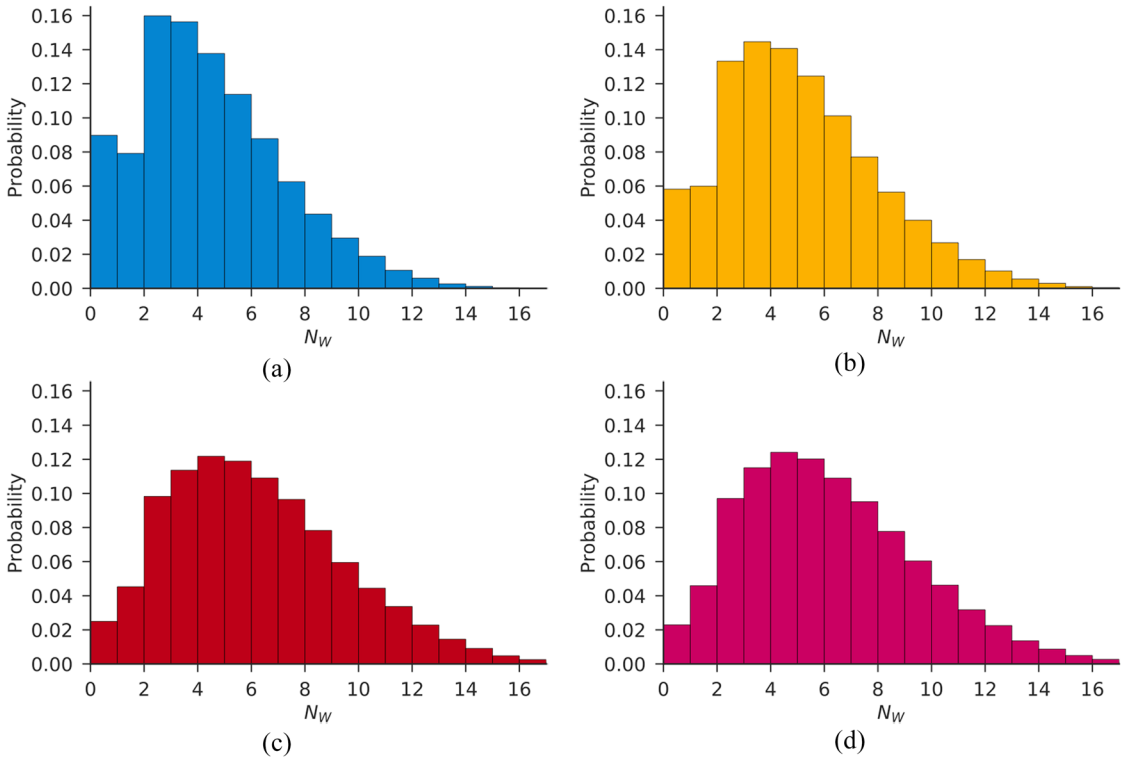

FIG. 12. Distributions of the minimum number of hydrogen bonded water molecules (N_w) that connect the (a) onium, (b) phosphate, (c) E1 ester, and (d) E2 ester groups on the C_3-PC lipid molecules to a propylene glycol molecule.

consistent with the $g(r)$s in Fig. 9. The other —OH group on the PG molecules shows similar hydration patterns to those shown in Fig. 10 for E1. Interestingly, the SDMs for the PG solvation of the second ester group (E2) show a similar solvation pattern for both MD and EPSR, shown in Fig. 11. While MD shows consistent solvation patterns independent of the ester or PG isomer, EPSR shows consistently different solvation of the C_3-PC ester groups which is dependent on the solvating isomer of PG. Specifically the R-isomer shows a solvation pattern similar to that of MD, and to the hydration of this group while the S-isomer shows a somewhat different and more diffuse distribution of PG molecules.

E. Topological analysis

In order to determine how the water molecules and PG molecules interact with one another around various portions of the PC headgroup, the solvation "topology" in the MD simulations has been assessed (see Sec. II D). This provides an assessment of how water molecules mediate the interactions between the PG molecules and the C_3-PC molecules in the MD system. Figure 12 shows the resultant distributions which give the probability that a PG molecule is connected to the onium, phosphate, and ester groups of the C_3-PC lipids via a certain number of hydrogen bonded water molecules (N_w). For instance, if a PG molecule is hydrogen bound to a water molecule which in turn is bound to another water molecule which is a first neighbor of the C_3-PC N atom, then $N_w = 2$.

The solvation distributions for the $N(CH_3)_3^+$ group are consistent with both the $g(r)$s and the SDMs in Fig. 4, in that there are relatively few direct interactions ($N_w = 0$) between the PG molecules and the onium headgroup. Even though these interactions are few in number, in Fig. 12(a) direct-PG interactions are more probable for the $N(CH_3)_3^+$ group than the phosphate or either of the ester groups on C_3-PC. Specifically for direct PC-PG contacts onium > phosphate > E2 ≈ E1, consistent with the coordination numbers reported in Tables III and V.

Given the relatively few PC-PG direct interactions, this graph theoretic approach allows the solvent network to be efficiently mapped within the systems in order to more accurately describe the location of the PG molecules around the headgroup. Further, from Fig. 12, the most probable locations of PG molecules show that they are closer to the onium headgroup (removed by two hydrogen-bonded water molecules) than either the phosphate (removed by three hydrogen-bonded water molecules) or the E1 and E2 ester (removed by 4 hydrogen bonded water molecules) groups. In fact, the distributions show that the probability that a propylene glycol is directly bound, or interacting with the onium headgroup through one or two mediating water molecules, is larger than the same scenarios with the phosphate or ester groups.

IV. CONCLUSIONS

In the solutions investigated here (30 mol. % PG in aqueous solution), the PG molecules seem to have a very limited effect on the hydration around different portions of the lipid headgroup. Interestingly, for each polar group in C_3-PC, water is preferred over PG despite the addition of this relatively large molecule to the mixture. While there is a reduction of the number of coordinated water molecules around each group compared to the hydration of the C_3-PC lipid in pure water,[12] there are relatively few PG interactions around each of the various parts of the lipid headgroup. Compared with the hydration of this lipid in DMSO/water mixtures (at the same mol. % as for PG here), there is a slightly lower reduction in the hydration interactions for the present solutions.[11] Further, the unique water hydrogen-bonding interaction to the $—CH_2—$ group directly below the $N(CH_3)_3^+$ motif is maintained even in the presence of the PG molecules. Whilst PG hydrogen bonds to this group and the PO_4^- group, the coordination numbers for these interactions are surprisingly low (Tables IV and V) given that there are 2 —OH groups on each PG molecule. While the EPSR fits to the neutron data show less PG-phosphate bonding compared with the MD simulations, in both simulations, the primary hydrogen bonding interaction is with water rather than the PG molecules. When PG does directly bind to C_3-PC, it seems to have a preference to bind onium > phosphate > E2 & E1, suggesting that the PG molecules will have a larger effect on the onium region of the headgroup than anywhere else on PC molecules. In a lipid bilayer arrangement, it has been shown that that there is a network of hydrogen bonds between the phosphate group and the onium group, sometimes mediated by a bridging water molecule.[43] In this environment, a competing solvation of the onium group may be enough to disrupt this network and enhance the permeability at the interfacial region.

The relative lack of PG interactions with other parts of the PC headgroup and largely unperturbed PC-water interactions may be due to the relative size of water molecules which are likely able to pack more closely to the onium and phosphate groups. The increased size of PG would naturally make it more difficult for this molecule to pack tightly around the groups and form strong bonds. By having no group that PG preferentially binds to on the PC headgroup could be an attributing factor that allows PG to more easily penetrate through a membrane environment as they would not become "stuck" to the polar parts of the lipid headgroups. Observation of the solvent structure suggests that PG does not perturb water structure,[9] and that the PG-solvent interactions are not affected by the addition of C_3-PC to the solution. This differs to studies of C_3-PC in DMSO/water solutions[11] where DMSO-water interactions were said to increase, which might be indicative of PG having a less perturbing effect as a solvent on lipid systems compared with DMSO.[44] That the hydration observed here is highly consistent with that observed for the DOPC headgroup in a bilayer,[41] which in turn is highly similar to the solvation of C_3-PC in solution,[12] suggests that the current measurements are significantly useful in determining the behavior of PG in membranes.

SUPPLEMENTARY MATERIAL

See supplementary material for SDMs and RDFs indicated in the main text.

ACKNOWLEDGMENTS

We thank the ISIS Facility (Rutherford Appleton Laboratories, STFC, UK) for the allocation of neutron beam time. S.E.M., N.H.R., and R.J.G. thank the UK Engineering and Physical Sciences Research Council (No. EP/J002615/1) and The Leverhulme Trust for research funding (No. RPG-2015-135). Additionally, R.M.Z. and C.D.L. acknowledge the research environment provided by the EPSRC Centre for Doctoral Training in Cross-Disciplinary Approaches to Non-Equilibrium Systems (CANES, No. EP/L015854/1). Finally, it is through C.D.L.'s membership within the UK HPC Materials Chemistry Consortium, which is funded by the Office of Science and Technology through the EPSRC High End Computing Programme (Grant No. EP/L000202), that the use of facilities of ARCHER, the UK National Supercomputing Service (http://www.archer.ac.uk), was possible for the Molecular Dynamics simulations presented in this work.

[1]Committee for Human Medicinal Products (CHMP), "Background review for the excipient propylene glycol," Technical Report No. EMA/CHMP/334655/2013, European Medicals Agency, 2014.
[2]A. Martino and E. Kaler, "The stability of lamellar phases in water, propylene glycol, and surfactant mixtures," Colloids Surf., A **99**, 91–99 (1995).
[3]H. Pfeiffer, H. Binder, G. Klose, and K. Heremans, "Hydration pressure and phase transitions of phospholipids," Biochim. Biophys. Acta, Biomembr. **1609**, 148–152 (2003).
[4]M. M. A. Elsayed, O. Y. Abdallah, V. F. Naggar, and N. M. Khalafallah, "PG-liposomes: Novel lipid vesicles for skin delivery of drugs," J. Pharm. Pharmacol. **59**, 1447–1450 (2007).
[5]R. D. Harvey, N. Ara, R. K. Heenan, D. J. Barlow, P. J. Quinn, and M. J. Lawrence, "Stabilization of distearoylphosphatidylcholine lamellar phases in propylene glycol using cholesterol," Mol. Pharmaceutics **10**, 4408–4417 (2013).
[6]C. Seguin, J. Eastoe, R. K. Heenan, and I. Grillo, "SANS studies of the effects of surfactant head group on aggregation properties in water/glycol and pure glycol systems," J. Colloid Interface Sci. **315**, 714–720 (2007).
[7]A. Soper, "Empirical potential Monte Carlo simulation of fluid structure," Chem. Phys. **202**, 295–306 (1996).
[8]N. Steinke, A. Genina, C. D. Lorenz, and S. E. McLain, "Salt interactions in solution prevent direct association of urea with a peptide backbone," J. Phys. Chem. B **121**, 1866–1876 (2017).
[9]N. H. Rhys, F. Bruni, S. Imberti, S. E. McLain, and M. A. Ricci, "Glucose and mannose: A link between hydration and sweetness," J. Phys. Chem. B **121**, 7771–7776 (2017).
[10]R. Hargreaves, D. T. Bowron, and K. Edler, "Atomistic structure of a micelle in solution determined by wide q-range neutron diffraction," J. Am. Chem. Soc. **133**, 16524–16536 (2011).
[11]A. Dabkowska, F. Foglia, M. Lawrence, C. Lorenz, and S. McLain, "On the solvation structure of dimethylsulfoxide/water around the phosphatidylcholine head group in solution," J. Chem. Phys. **135**, 225105 (2011).
[12]F. Foglia, M. J. Lawrence, C. D. Lorenz, and S. E. McLain, "On the hydration of the phosphocholine headgroup in aqueous solution," J. Chem. Phys. **133**, 145103 (2010).
[13]J. McGregor, R. Li, J. A. Zeitler, C. D'Agostino, J. H. P. Collins, M. D. Mantle, H. Manyar, J. D. Holbrey, M. Falkowska, T. G. A. Youngs, C. Hardacre, E. H. Stitt, and L. F. Gladden, "Structure and dynamics of aqueous 2-propanol: A THz-TDS, NMR and neutron diffraction study," Phys. Chem. Chem. Phys. **17**, 30481–30491 (2015).
[14]E. Scoppola, A. Sodo, S. E. McLain, M. A. Ricci, and F. Bruni, "Water-peptide site-specific interactions: A structural study on the hydration of glutathione," Biophys. J. **106**, 1701–1709 (2014).
[15]A. Sridhar, A. J. Johnston, L. Varathan, S. E. McLain, and P. C. Biggin, "The solvation structure of alprazolam," Phys. Chem. Chem. Phys. **18**, 22416–22425 (2016).
[16]N. H. Rhys, R. J. Gillams, L. E. Collins, S. K. Callear, M. J. Lawrence, and S. E. McLain, "On the structure of an aqueous propylene glycol solution," J. Chem. Phys. **145**, 224504 (2016).
[17]M. Kohagen, P. E. Mason, and P. Jungwirth, "Accurate description of calcium solvation in concentrated aqueous solutions," J. Phys. Chem. B **118**, 7902–7909 (2014).
[18]S. Soffientini, L. Bernasconi, and S. Imberti, "The hydration of formic acid and acetic acid," J. Mol. Liq. **205**, 85–92 (2015), Global Perspectives on the Structure and Dynamics of Liquids and Mixtures: Experiment and Simulation 9-13 September 2013.
[19]S. E. Norman, A. H. Turner, J. D. Holbrey, and T. G. A. Youngs, "Solvation structure of uracil in ionic liquids," ChemPhysChem **17**, 3923–3931 (2016).
[20]J. Towey, A. Soper, and L. Dougan, "Molecular insight into the hydrogen bonding and micro-segregation of a cryoprotectant molecule," J. Phys. Chem. B **116**, 13898–13904 (2012).
[21]A. J. Johnston, Y. R. Zhang, S. Busch, L. C. Pardo, S. Imberti, and S. E. McLain, "Amphipathic solvation of indole: Implications for the role of tryptophan in membrane proteins," J. Phys. Chem. B **119**, 5979–5987 (2015).
[22]C. Hardacre, S. E. J. McMath, M. Nieuwenhuyzen, D. T. Bowron, and A. K. Soper, "Liquid structure of 1, 3-dimethylimidazolium salts," J. Phys.: Condens. Matter **15**, S159 (2003).
[23]J. Hladílková, H. E. Fischer, P. Jungwirth, and P. Mason, "Hydration of hydroxyl and amino groups examined by molecular dynamics and neutron scattering," J. Phys. Chem. B **119**, 6357–6365 (2015).
[24]V. Sears, "Neutron scattering lengths and cross sections," Neutron News **3**, 26–37 (1992).
[25]A. Soper, "GudrunN and GudrunX: Programs for correcting raw neutron and x-ray diffraction data to differential scattering cross section," Technical Report No. RAL-TR-201, 2011.
[26]S. E. McLain, C. J. Benmore, J. E. Siewenie, J. Urquidi, and J. F. C. Turner, "On the structure of liquid hydrogen fluoride," Angew. Chem., Int. Ed. **43**, 1952–1955 (2004).
[27]J. B. Klauda, R. M. Venable, J. A. Freites, J. W. O'Connor, D. J. Tobias, C. Mondragon-Ramirez, I. Vorobyov, A. D. MacKerell, Jr., and R. W. Pastor, J. Phys. Chem. B **114**, 7830–7843 (2010).
[28]K. Vanommeslaeghe, E. Hatcher, C. Acharya, S. Kundu, S. Zhong, J. Shim, E. Darian, O. Guvench, P. Lopes, I. Vorobyov, and A. D. MacKerell, Jr., "CHARMM general force field: A force field for drug-like molecules compatible with the CHARMM all-atom additive biological force fields," J. Comput. Chem. **31**, 671–690 (2010).
[29]H. Berendsen, J. Grigera, and T. Straatsma, "The missing term in effective pair potentials," J. Phys. Chem. **91**, 6269–6271 (1987).
[30]W. L. Jorgensen, J. Chandrasekhar, J. D. Madura, R. W. Impey, and M. L. Klein, "Comparison of simple potential functions for simulating liquid water," J. Chem. Phys. **79**, 926–935 (1983).
[31]J. P. Ryckaert, G. Ciccotti, and H. J. C. Berendsen, J. Comput. Phys. **23**, 327 (1977).
[32]S. Plimpton, J. Comput. Phys. **117**, 1 (1995).
[33]R. W. Hockney and J. W. Eastwood, *Computer Simulation Using Particles* (Adam Hilger, New York, 1988).
[34]A. Luzar and D. Chandler, J. Chem. Phys. **98**, 8160 (1993).
[35]A. A. Hagberg, D. A. Schult, and P. J. Swart, "Exploring network structure, dynamics, and function using networkX," in *Proceedings of the 7th Python in Science Conference (SciPy2008)*, G. Varoquaux, T. Vaught, and J. Millman (Eds.), pp. 11–15.
[36]See https://gcm.upc.edu/en/members/luis-carlos/angula/ANGULA.
[37]S. Busch, C. Lorenz, J. Taylor, L. Pardo, and S. McLain, "Short-range interactions of concentrated proline in aqueous solution," J. Phys. Chem. B **118**, 14267–14277 (2014).
[38]S. Busch, L. Pardo, W. O'Dell, C. Bruce, C. Lorenz, and S. McLain, "On the structure of water and chloride ion interactions with a peptide backbone in solution," Phys. Chem. Chem. Phys. **15**, 21023–21033 (2013).
[39]S. E. McLain, A. K. Soper, and A. Luzar, "Investigations on the structure of dimethyl sulfoxide and acetone in aqueous solution," J. Chem. Phys. **127**, 174515 (2007).
[40]A. P. Dabkowska, M. J. Lawrence, S. E. McLain, and C. D. Lorenz, "On the nature of hydrogen bonding between the phosphatidylcholine head group and water and dimethylsulfoxide," Chem. Phys. **410**, 31–36 (2013).

[41]R. J. Gillams, C. D. Lorenz, and S. E. McLain, "Comparative atomic-scale hydration of the ceramide and phosphocholine headgroup in solution and bilayer environments," J. Chem. Phys. **144**, 225101 (2016).
[42]E. C. Hulme, A. K. Soper, S. E. McLain, and J. L. Finney, Biophys. J. **91**, 2371–2380 (2006).
[43]M. Pasenkiewicz-Gierula, Y. Takaoka, H. Miyagawa, K. Kitamura, and A. Kusumi, "Hydrogen bonding of water to phosphatidylcholine in the membrane as studied by a molecular dynamics simulation: Location, geometry, and lipidlipid bridging via hydrogen-bonded water," J. Phys. Chem. A **101**, 3677–3691 (1997).
[44]C. J. Malajczuk, Z. E. Hughes, and R. L. Mancera, "Molecular dynamics simulations of the interactions of DMSO, mono- and polyhydroxylated cryosolvents with a hydrated phospholipid bilayer," Biochim. Biophys. Acta **1828**, 2041–2055 (2013).